TESTS OF THE WEAK NEUTRAL CURRENT IN ep COLLISIONS AT HIGH Q^2

F. E. Taylor
Physics Department
Northern Illinois University
DeKalb, Illinois 60115

Abstract

The very high Q^2 values offered by an e-p collider allow various stringent tests of the theory of the weak neutral current to be made. These tests permit a determination of the Z^o - mass through propagator effects and a determination of $\sin^2\theta_w$ through e-p scattering with polarized electron beams. The statistical precision of these tests are reviewed and various experimental cuts which guarantee an unambiguous confrontation of the standard model are discussed.

(I) Introduction:

The famous SLAC e-D scattering with a polarized electron beam established the interference of the electromagnetic scattering amplitude with the neutral current weak amplitude[1]. The results of this experiment are consistent with the standard SU(2)xU(1) model of weak interactions, and serve to rule out models in which the vector and axial currents are exchanged from the usual assignments. This result is interpreted as an important confirmation of the standard gauge model[2].

However several theorists, including Bjorken[3], have emphasized that the low Q^2 phenomenology of the standard SU(2)xU(1) model can be reproduced without a unification of the electromagnetic and the weak interactions. Hung and Sakurai[4] have observed that both the form and the strength of the neutral current follow simply from the calculation of the γ-Z^o mixing if the following conditions are satisfied:

1. The photon is massless before and after mixing.
2. The theory of weak interactions is SU(2) invariant and pure V-A before mixing.

With these conditions, they have reproduced all the low energy neutral current phenomenology.

In this alternative view the parameter "$\sin^2\theta_w$" can be derived as a radiative correction and will consequently have a Q^2 - dependence which would become important in the high Q^2 range $Q^2 \sim M^2_{Z^o}$. This point of view has been stressed by Dombey[5]. Hence it is important to measure both $\sin^2\theta_w$ at high Q^2, and separately determine the values of intermediate boson masses M_{Z^o} and $M_{W^\pm}$ to test this alternative theory.

The parameters $\sin^2\theta_w$ and M_{Z^o} can be measured in an e-p collider by computing various asymmetry parameters which follow from different ep scattering cross sections for electrons and positrons which are polarized left-handed or right-handed. For $Q^2 < M^2_{Z^o}$, the Z^o propagator effects in the γ-Z^o interference term and in the weak term in the ep cross section make these terms grow relative to the electromagnetic cross section term with increasing Q^2. Hence the weak neutral current effects become relatively large at high Q^2 making the measurements at high Q^2 a much more sensitive test of the weak neutral current.

In this paper various asymmetries are analyzed in terms of their power to confront the theory. There are many discussions of these asymmetry ratios in the various e-p collider proposals[6]. Here we attempt to make a systematic comparison of the power of these various tests as a function of the integrated luminosity and Q^2 range. Attention is paid to various experimental corrections, such as the QED one photon - two photon interference effects which can distort certain asymmetries intended to measure electro-weak effects.

II. The Cross Section:

The ep scattering cross section at high Q^2 can be written as (assuming the Callan-Gross relation):

$$\frac{4\pi}{s}\frac{d\sigma}{dxdy} = |\gamma|^2 + (\gamma\text{-}z) + |z|^2 \qquad (1)$$

where:

$$|\gamma|^2 = \frac{e^4}{Q^4} f^+ F_2^{em}$$

$$(\gamma\text{-}z) = \frac{e^2}{Q^2}\,\frac{2\sqrt{2}}{(1+Q^2/M^2_{Z^o})}\,G_F\,g_\eta\left[f^+F_2^{int} + \xi_\eta\, f^- xF_3^{int}\right]$$

$$|Z|^2 = \frac{2\,G_F^2}{(1+Q^2/M_Z^2)^2}\; g_\eta^2 \left[f^+ F_2^{wk} + \xi_\eta\, f^-\, x\, F_3^{wk}\right]$$

$$f^+ = \frac{1+(1-y)^2}{2} \text{ and } f^- = \frac{1-(1-y)^2}{2}$$

$$M_{Z^o} = 37.4/\sin^2\theta_w\cos^2\theta_w,\; M_W^{\pm} = 37.4/\sin^2\theta_w$$

The assignments of the coupling constants g_η and ξ_η are given in the following Table .

Table I

	Left-handed	Right-handed
ξ_η	+1	-1

The weak couplings of the incoming lepton:

	g_L	g_R
	e_L^- e_R^+	e_R^- e_L^+
g_η	$1-2\sin^2\theta_w$	$-2\sin^2\theta_w$

The quark couplings:

	charge	g_{q_l}
left handed	+2/3	$1-4/3\sin^2\theta_w$
	-1/3	$2/3\sin^2\theta_w - 1$
	charge	g_{q_r}
right handed	+2/3	$-4/3\sin^2\theta_w$
	-1/3	$2/3\sin^2\theta_w$

Finally the structure functions are given by:

$$F_2^{em} = \sum_q Q_q^2 \left(q(x) + \bar{q}(x)\right)$$

$$F_2^{int} = \sum_q 1/2\,(g_{ql} + g_{qr})\, Q_q \left(q(x) + \bar{q}(x)\right)$$

$$xF_3^{int} = \sum_q 1/2\,(g_{ql} - g_{qr})\, Q_q \left(q(x) - \bar{q}(x)\right)$$

$$F_2^{wk} = \sum_q 1/2\,(g_{ql}^2 + g_{qr}^2)\left(q(x) + \bar{q}(x)\right)$$

$$xF_3^{wk} = \sum_q 1/2\,(g_{ql}^2 - g_{qr}^2)\left(q(x) - \bar{q}(x)\right)$$

The deep inelastic scattering is described by 3 parity conserving structure functions F_2^{em}, F_2^{int} and F_2^{wk} and by 2 parity violating structure functions xF_3^{int} and xF_3^{wk}. By varying the charge and polarization of the incoming lepton, the various weak cross section terms can be isolated.

There are two main interests in studying these weak terms 1) to determine the mass of the Z^o boson through a measurement of the Q^2 - dependence of the γ-Z^o interference terms, and 2) a determination of $\sin^2\theta_w$ at high Q^2 by measuring the magnitude of various left-right asymmetries. There is a third interest in that it is theoretically possible to extract the parity violating structure function xF_3^{int} as well as measuring F_2^{em} by considering various sums and differences of cross sections. However the experimental errors of this procedure are large.

To see the order of magnitude of these various terms in the cross section, the electromagnetic term $|\gamma|^2$ and the e_L^- weak interference and weak terms are plotted in figure 1 for 4-energy ranges: SLAC $s=37.5$ GeV^2, FNAL-Tevatron II μ beam $s=1126$ GeV^2, ep collider (10 GeV x 1 TeV) $s=4\times10^4$ GeV^2, and a super ep collider 100 GeV x 20 TeV $s=8\times10^6$ GeV^2. At SLAC energies, the weak term is on the order of $\leq$ 0.1%, FNAL ~1%, ep collider 10%, super ep collider ~30%. Note that in this figure $4\pi/s\; d\sigma/dxdy$ is plotted versus Q^2 for fixed x and s and thus $y=Q^2/sx$ is varying with Q^2. From these curves we see that the weak and interference terms grow relative to the electromagnetic term with increasing Q^2, but at the super ep collider, the propagator effects saturate thereby giving all cross section terms a $1/Q^4$ dependence. Thus no further enhancement of the weak terms is possible for $Q^2 >> m_{Z^o}^2$ (except for y-dependent effects near the kinematic boundary).

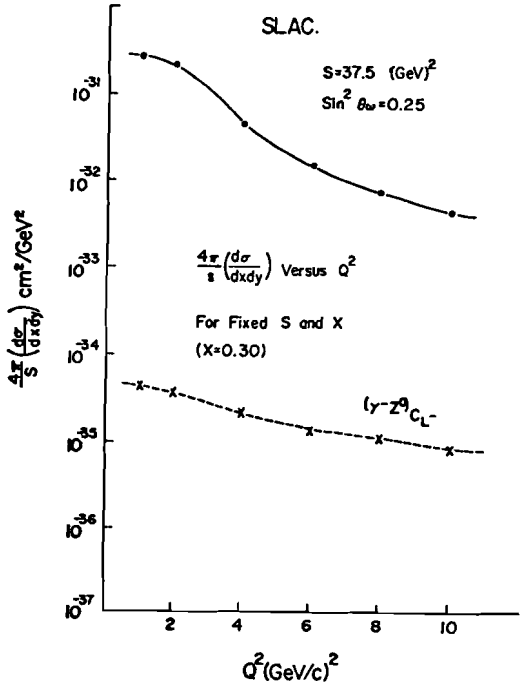

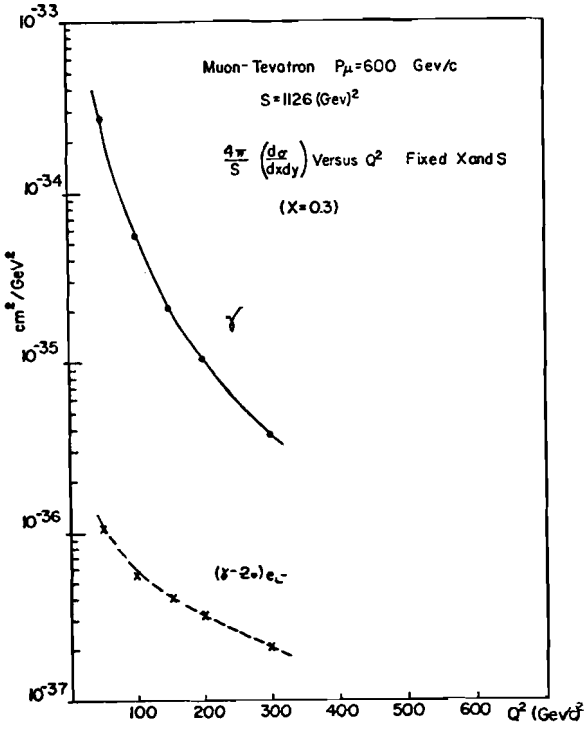

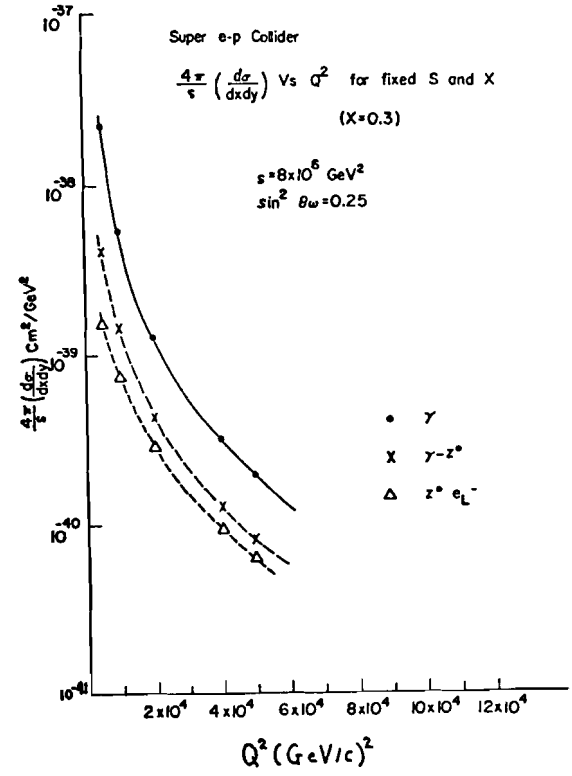

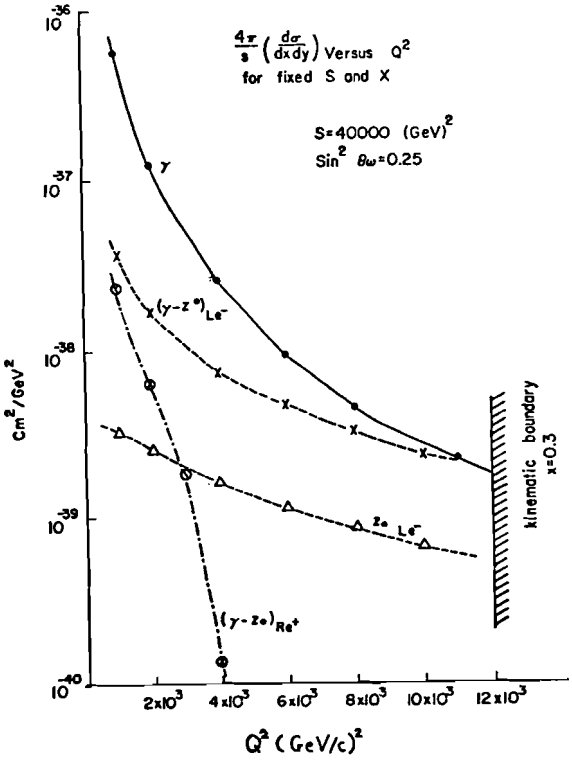

Figure 1: The cross section $4\pi/s\ d\sigma/dxdy$ versus Q^2 for fixed x=0.3 and for $\sin^2\theta_w=0.25$ for various values of S. The pure electromagnetic term $|\gamma|^2$ and the electroweak term $|\gamma-Z|$ for left handed electrons is shown.

(III) The Asymmetries:

The cross section asymmetries are of two classes: those involving polarized electron beams and the one which does not.

a) The charge asymmetry

The difference between unpolarized electron-proton scattering isolates the z^o propagator effect, and the ratio of xF_3^{int}/F_2^{em}. Since the beam is unpolarized in this test the measured cross sections are:

$$\sigma_- = (\sigma_{-L} + \sigma_{-R})/2$$

$$\sigma_+ = (\sigma_{+L} + \sigma_{+R})/2$$

thus:

$$A_{ch} = \frac{\sigma_- - \sigma_+}{\sigma_- + \sigma_+} = \frac{\sqrt{2}\,G_F\,Q^2}{(1+Q^2/m_{Zo}^2)e^2}\,\frac{f^-}{f^+}\,\frac{xF_3^{int}}{F_2^{em}} \qquad (3)$$

This ratio is plotted in figure 2 as a function of x for various values of Q^2 for the ep collider at s=40,000 Gev^2. The Buras and Gaemers[7] parameterization was used. It is evident that this asymmetry has a large x-dependence as well

as a large Q^2 dependence. The x-dependence comes from the ratio xF_3^{int}/F_2^{em} where $xF_3^{int} \sim q(x)-\bar{q}(x)$ and $F_2 \sim q(x)+\bar{q}(x)$, which strongly differ at $x<0.2$, and from the term:

$$\frac{f^-}{f^+} = \frac{1-(1-\frac{Q^2}{sx})^2}{1+(1-\frac{Q^2}{sx})^2} .$$

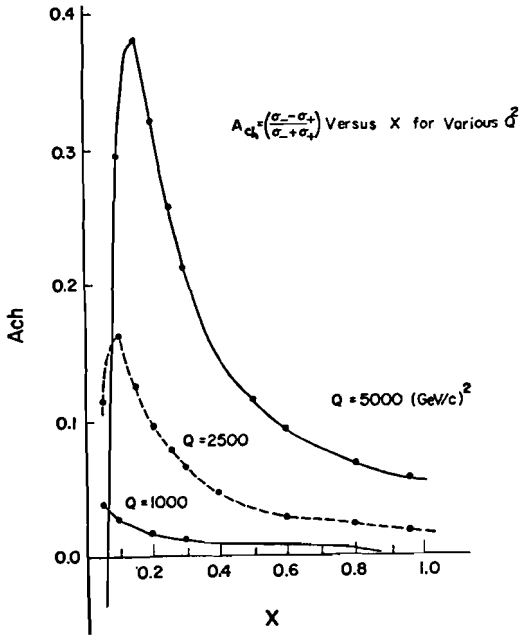

Figure 2: The charge asymmetry A_{ch} versus X for various values of Q^2. Note the strong X dependence. here s=40000 GeV^2 and $\sin^2\theta_w$=0.25.

Since the interest here is to measure the Q^2-dependence of this ratio to determine the Z^o propagator effect, we define a new ratio:

$$\bar{A}_{ch}(Q^2) \equiv \left(\frac{\sigma_- - \sigma_+}{\sigma_- + \sigma_+}\right)\frac{f^+}{f^-} \simeq \frac{\sqrt{2}G_F}{e^2}\,\frac{XF_3^{int}}{F_2^{em}}\,\frac{Q^2}{\left(1+\frac{Q^2}{m_Z^2}\right)} \qquad (4)$$

By choosing a minimum observed value of x such that $\bar{q}(x) \ll q(x)$, the x-dependence of this ratio will be small. There is a complicating Q^2-dependence in addition to the propagator term which arises from QCD effects. From QCD theory, to leading order, $XF_3^{int}(X,Q^2)$ can evolve by only gluon radiation and $F_2^{em}(X,Q^2)$ is sensitive to both gluon radiation and quark-antiquark pair production. Since most of the quark-antiquark pair production produces a strong Q^2-dependence at low x, the x min cut above should suffice. From the parameterization of Buras and Gaemers $X_{min} \simeq 0.2$. Finally we note that this ratio is sensitive to $\sin^2\theta_w$, since:

$$XF_3^{int} \propto (g_{ql} - g_{qr})\,(q - \bar{q})$$

where $g_{ql} - g_{qr}$ has no $\sin^2\theta_w$ dependence. The charge asymmetry given by equation (4) is plotted in figure 3 for a fixed value of $\sin^2\theta_w$=0.25 for various values of m_{Z^o}.

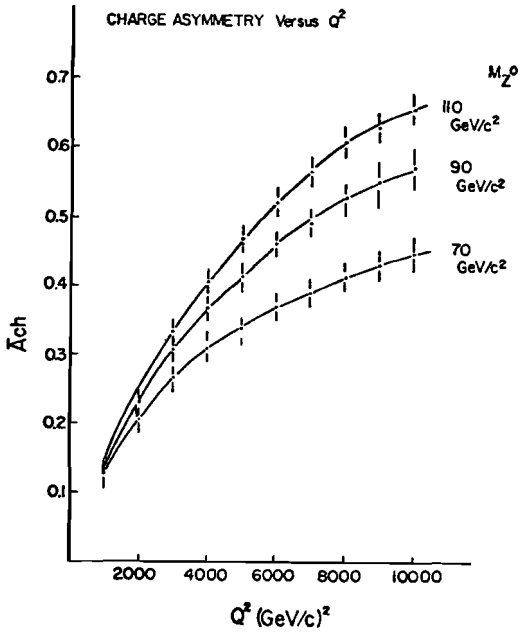

Figure 3: The modified charge asymmetry $\bar{A}_{ch}$ averaged over $0.2 \leq x \leq 1.0$ for various values of M_{Z^o} versus Q^2. The error bars are for an integrated luminosity of 5×10^{39}/cm^2 for each lepton sign.

b) Polarized Beam Asymmetries:

There are approximately 16 asymmetry ratios involving cross section sums and differences which can be measured with an ep collider with electrons and positrons, polarized left handed or right handed. Of these many possibilities, only asymmetries of the type (difference/difference) or (sum/sum) have no XF_3^{int}/F_2^{em} component and require no X_{min} cut discussed above. Asymmetries of the type (a-b)/(a+b) have a term proportional to $(q(x)-\bar{q}(x))/(q(x)+\bar{q}(x))$ which involves an explicit X-dependence at low $X<0.2$ and thus requires a $X \geq X_{min} \sim 0.2$ cut to be free of this X-dependence and low x QCD Q^2 dependence discussed above.

To measure the weak neutral current effects consider the ratio:

$$A_{dLR} = \frac{\sigma_{eL^-} - \sigma_{eR^+}}{\sigma_{eR^-} - \sigma_{eL^+}} \simeq \frac{-g_L}{g_R}\left[1 + \frac{Q^2}{\left(1+\frac{Q^2}{m_{Z^o}^2}\right)}\,\frac{G_F}{\sqrt{2}e^2}\,\frac{XF_3^{wk}}{XF_3^{int}}\right] \qquad (5)$$

and for $\sin^2\theta_w \sim 3/8$, XF_3^{wk} becomes very small and thus A_{dLR} has little Q^2 dependence. For low Q^2, the Q^2 dependent term is small and thus

$$A_{dLR} \cong \frac{1-2\sin^2\theta_w}{2\sin^2\theta_w} . \qquad (6)$$

Hence this ratio can be used to determine $\sin^2\theta_w$ as plotted in figure 4. However, the errors in this ratio can be quite large owing to the small difference of cross sections in the denominator and to radiation effects which add when the difference $e^- - e^+$ is taken. The error analysis of this is discussed later.

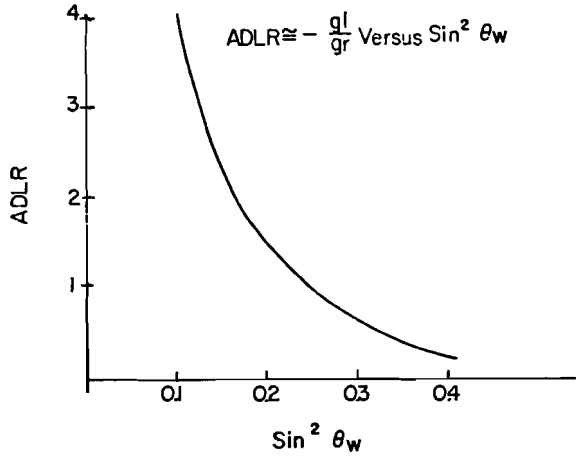

Figure 4: The asymmetry A_{dLR} versus $\sin^2\theta_w$ for $Q^2=0$.

The third asymmetry we consider the left-right asymmetry of $e^{\mp}$-p scattering:

$$A_{LRe^{\mp}} \equiv \frac{\sigma_{L}^{\mp} - \sigma_{R}^{\mp}}{\sigma_{L}^{\mp} + \sigma_{R}^{\mp}} \qquad (7)$$

$$\cong \frac{\sqrt{2}\,G_F}{e^2}\,\frac{Q^2}{1+\frac{Q^2}{\overline{M}_{Z^o}^2}}\left[\pm(g_L-g_R)\,\frac{F_2^{int}}{F_2^{em}} + (g_L+g_R)\frac{f^-}{f^+}\,\frac{XF_3^{int}}{F_2^{em}}\right]$$

This ratio has an x-dependence for small x through the second term, as well as a Q^2 dependence from the propagator term. Referring to the cross section terms described above we have:

$$A_{LRe^{\pm}} \cong \frac{\sqrt{2}\,G_F}{e^2}\,\frac{Q^2}{(1+\frac{Q^2}{\overline{m}_{Z^o}^2})}\left[\pm\frac{F_2^{int}}{F_2^{em}} + (1-4\sin^2\theta_w)\frac{f^-}{f^+}\,\frac{XF_3^{int}}{F_2^{em}}\right] \qquad (8)$$

Hence there is an explicit dependence on $\sin^2\theta_w$ and this ratio can in principle be used to independently determine m_{Z^o} and $\sin^2\theta_w$. These asymmetries are plotted in figure 5 as a function of x and Q^2.

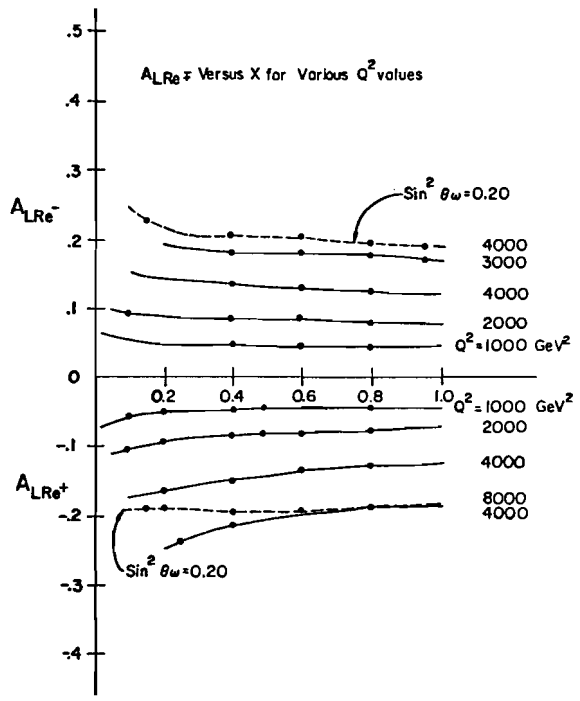

Figure 5: The asymmetry $A_{LRe\pm}$ versus x for various Q^2. The solid curves are for $\sin^2\theta_w=0.25$ and the dotted curves are for $\sin^2\theta_w=0.20$ at $Q^2=4000\,(GeV/c)^2$.

The fourth asymmetry we consider involves sums of polarized electron and polarized positron cross sections. This has the advantage of not being sensitive to radiative effects to be discussed later. We define:

$$A_{SLR} \equiv \frac{\sigma_{e^-L} + \sigma_{e^+R}}{\sigma_{e^-R} + \sigma_{e^+L}}$$

$$\cong 1 + \frac{2\sqrt{2}\,G_F}{e^2}\,\frac{Q^2}{(1+\frac{Q^2}{\overline{m}_{Z^o}^2})}\,\frac{F_2^{int}}{F_2^{em}}\,(g_L-g_R) \qquad (9)$$

In the standard model $(g_L-g_R)=1$, and

$$F_2^{int} \approx 1/3(1-8/3\,\sin^2\theta_w)\,[q_{2/3}(x)+\bar{q}_{2/3}(x)] - 1/6(4/3\,\sin^2\theta_w-1)\,[q_{-1/3}(x)+\bar{q}_{-1/3}(x)]\ .$$

Hence in this ratio there is a sensitivity to both m_{Z^o} and $\sin^2\theta_w$ and will have a diminishing sensitivity to m_{Z^o} as $\sin^2\theta_w \to 3/8$ through the F_2^{int} term. We plot this ratio in figure 6 for various values of m_{Z^o} at $\sin^2\theta_w=0.25$, and in figure 7 for various values of $\sin^2\theta_w$ for fixed $m_{Z^o}=90\ GeV/c^2$.

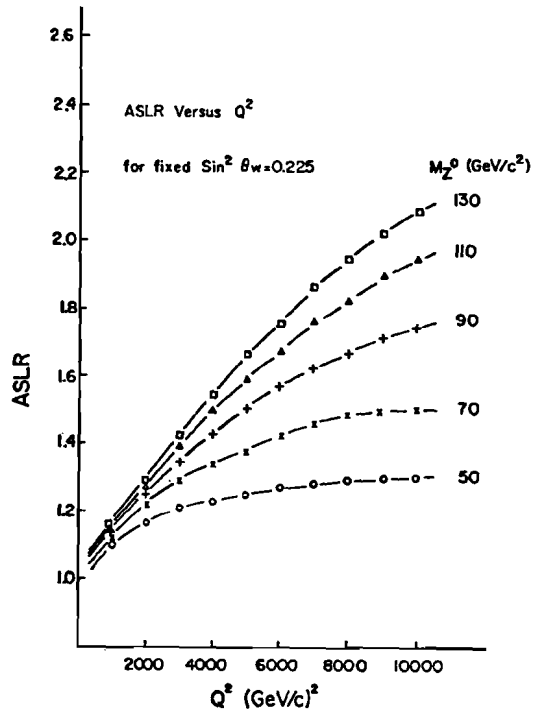

Figure 6: The ratio A_{SLR} versus Q^2 for fixed $\sin^2\theta_w$=0.225 for various Z^0 masses. This illustrates the dependence on the mass M_{Z^0}.

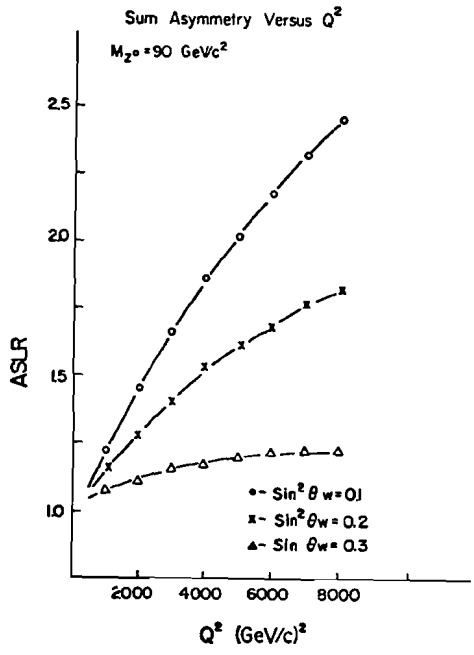

Figure 7: The ratio A_{SLR} versus Q^2 for various values of $\sin^2\theta_w$ at a fixed M_{Z^0}=90 GeV/c^2 showing the dependence on $\sin^2\theta_w$.

(IV). Radiative Effects:

Sizable corrections to asymmetries involving electron-positron differences come from the interference between one and two photon exchange. The sign of this interference follows the sign of the incoming lepton and will cancel in sums of electron and positron cross sections, but will add with differences. The cross section from this interference effect has been calculated by Gorshkov[8], Bartels[9], and Fishbane and Kinsley[10] and is given by:

$$\frac{4\pi}{s}\frac{d\sigma}{dxdy}(2\gamma)\underset{e_+}{=}\mp\frac{3}{2}\frac{\alpha}{2\pi}\ln^2\left(\frac{Q^2}{m^2}\right)\left(\frac{e^4}{Q^4}\right)f^+F_2(2\gamma) \qquad (10)$$

where:

$$F_2(2\gamma)=\Sigma\left(Q^3_{q_i}\,q_i(x,Q^2)+Q^3_{\bar{q}_i}\,\bar{q}_i(x,Q^2)\right) \qquad (11)$$

The parameter m is the reduced electron-quark mass and is not precisely known. As a rough guide we take m=0.3 GeV/c^2. Hence:

$$R(2\gamma)=\frac{\sigma(2\gamma)}{\sigma(1\gamma)}\cong\mp\frac{3}{2}\frac{\alpha}{2\pi}\ln^2\left(\frac{Q^2}{m^2}\right)\frac{2}{3} \qquad (12)$$

$$\cong\mp 1.2\times10^{-3}\ln^2\left(\frac{Q^2}{0.09}\right)$$

For Q^2=5000(GeV/c)^2, R(2γ)=14%, and for $Q^2=10^6$(GeV/c)^2, R(2γ)=31%. Thus the radiative effect is comparable to the asymmetry from weak-electromagnetic interference and can therefore significantly distort the observed asymmetries. To illustrate the importance of this effect, we plot in figure 8 the charge asymmetry given by equation 4 above with the radiative term. With such a severe distortion as observed in this figure, we must make a large correction, and the errors in this correction can strongly influence the error in determining M_{Z^0}.

To separate the radiative asymmetry from the weak-electromagnetic interference asymmetry we calculate:

$$A_{ch}=\frac{\sigma_- - \sigma_+}{\sigma_- + \sigma_+}\cong\frac{\sqrt{2}\,G_F}{e^2}\frac{Q^2}{(1+Q^2)\overline{m^2_{Z^0}}}\left(\frac{Q^2}{sx}\right)\frac{xF_3^{int}}{F_2^{em}}-\frac{3\alpha}{4\pi}\ln^2\left(\frac{Q^2}{m^2}\right)\frac{F_2^{int}}{F_2^{em}}$$

Thus as $Q^2\to 0$, we have:

$$A_{ch}\cong-\frac{3}{4}\frac{\alpha}{\pi}\ln^2\left(\frac{Q^2}{m^2}\right)\frac{F_2(2\gamma)}{F_2^{em}} \qquad (13)$$

To determine the unknown parameter m, we can plot the term:

$$\left(-\frac{4\pi}{3\alpha}A_{ch}\frac{F_2^{em}}{F_2(2\gamma)}\right)^{1/2}=\ln Q^2-\ln m^2 \qquad (14)$$

versus $\ln Q^2$ which has an intercept which estimates m. The errors associated with this process are discussed in the following section.

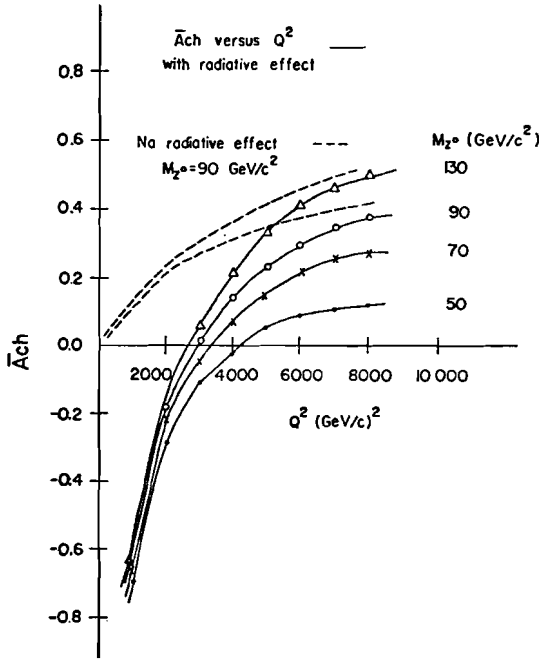

Figure 8: The charge asymmetry $\bar{A}_{ch}$ with and without radiative corrections. The radiative effect is amplified a low Q^2 by the term $f^+/f^- \cong sx/Q^2$ for small Q^2.

(V) Experimental Considerations:

Here we consider the power of various ratios to determine the Z^o mass through the propagator term and the value of $\sin^2\theta_w$ from the magnitude of the asymmetry at a fixed Q^2. The conditions of a real experiment are simulated by fixing s and the integral luminosity. No experimental resolutions are considered and no backgrounds other than the radiative effects discussed above are simulated. Hence these calculations are intended to represent the statistical limit of a "perfect" experiment. We use the parameterization of Buras and Gaemers with $\Lambda^2=0.1$ and $Q_o^2=1.8$ GeV^2. We also neglect the strange and charm sea. Because we are interested in the Q^2 dependence of the various ratios, we calculate:

$$N \text{ events } (x,Q^2) = \frac{d\sigma}{dxdQ^2}\,\Delta x \Delta Q^2 \int (L\Delta t)$$

where

$$\frac{d\sigma}{dxdQ^2} = \left(\frac{1}{sx}\right) \frac{d\sigma}{dxdy}$$

We take $s=40{,}000$ GeV^2 corresponding to a 10 GeV $e^{\pm}$ x 1 TeV p collider. Because most of the effects of interest are Q^2 dependent, the particular value of s is not of great importance. The most significant experimental consideration is the requirement of high luminosity at high $Q^2 \approx 6000(\text{GeV/c})^2$, where the propagator effects become important.

1) Determination of the Radiative Correction:

We have seen that the interference term between one photon and two photon exchange leads to a sizable asymmetry between e^--p scattering and e^+-p scattering. Thus it is important to accurately estimate this effect in the determination of M_{Z^o}. Additional radiative corrections arise from bremsstrahlung from the incident lepton and tend to "soften" the Q^2 distribution which can also introduce an error in M_{Z^o}.

In calculating the one photon-two photon exchange term discussed above, there are two tasks: 1) determine the value of m in the log term, and 2) estimate the structure function $F_2(2\gamma)$.

The determination of m depends on the approximation of $F_2(2\gamma)$. We therefore estimate this structure function first. By equation (11), we have to leading order:

$$F_2(2\gamma) \approx \left(\frac{2}{3}\right)^3 (q_{2/3}+\bar{q}_{2/3}) - \left(\frac{1}{3}\right)^3 (q_{-1/3}+\bar{q}_{-1/3})$$
$$\approx \frac{1}{2}\, F_2^{em}$$

The accuracy of this approximation is indicated in figure 9, where we see that for $x\sim 0.2$, $F_2(2\gamma)=1/2\ F_2^{em}$ to within 8%.

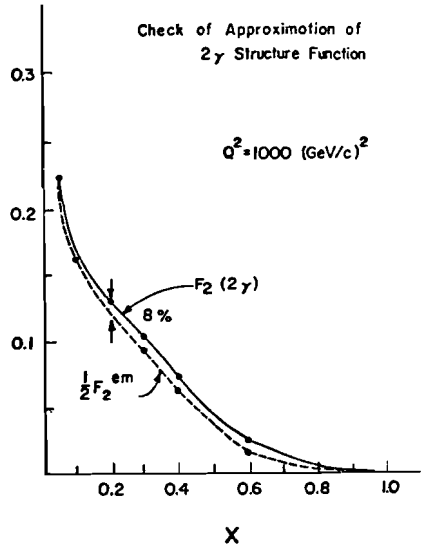

Figure 9: Check of the accuracy of the 2γ structure function approximation. $Q^2=1000(\text{GeV/c})^2$ and the parameterization of Buras and Gaemers has been used.

We use this approximation of $F_2(2Y)$ to estimate the parameter m. By equation (14):

$$\left(\frac{-8\pi}{3\alpha} A_{ch}\right)^{1/2} \cong \ln Q^2 - \ln m^2$$

The parameter m is estimated by plotting the term $\left(\frac{-8\pi}{3\alpha}A_{ch}\right)^{1/2}$ versus $\ln Q^2$. This is shown in figure 10 for $40 \leq Q^2 \leq 400$ (GeV/c)^2. For $Q^2 \geq 400$ (GeV/c)^2, equation (14) is no longer valid, because weak effects start to contribute for m~0.3 GeV/c^2. Values of $Q^2 < 40$ (GeV/c)^2 are not considered since higher twists can become large at low Q^2. Performing a least squares fit to the "data", we determine m=0.26$\pm$0.05 GeV/c^2 for an assumed value of m=0.3 GeV/c^2 for an integrated luminosity of 10^{38}/cm^2.

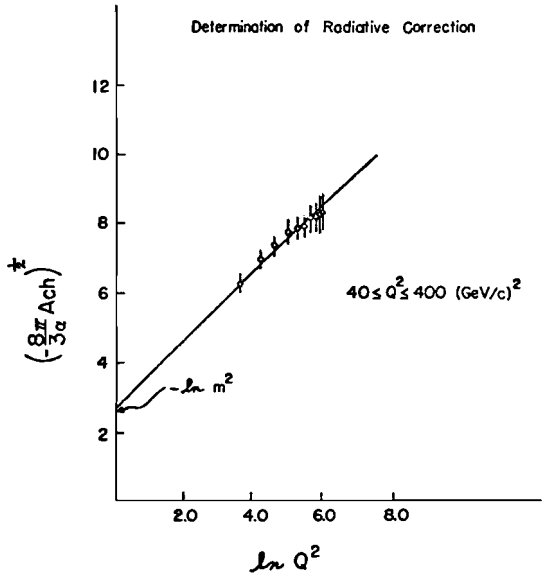

Figure 10: Determination of the radiative correction. The ordinate should be linear in $\ln Q^2$, and have an intercept of $-\ln m^2$.

We then correct the measured cross sections by this approximate radiative term. The error of the correction is approximately 5% for small x~0.05 and grows to ~30% for x~0.75. Since the radiative term is typically $\leq$10% of the cross section, the resulting error in the cross section is typically 3%. However the error in the asymmetry can be much larger depending on the values of x and Q^2. It must be emphasized that the measurement at low $Q^2 \leq 400$ (GeV/c)^2 is essential to the determination of this radiative correction and the design of the detector should accomodate this requirement.

2) Measurement of M_{z^o}:

The charge asymmetry defined by equation 4 corrected for the radiative effect discussed above, has a weak x-dependence for $x > 0.2$, but has a strong x-dependence and a possible strong Q^2-dependence in the low x region $x \leq 0.2$. For these reasons, we consider only $x > 0.2$ and compute the weighted average over $x \geq 0.2$ of the charge asymmetry for fixed Q^2 to determine the Q^2-dependence of the propagator term. Note that for a fixed s, the low x region is inaccessible at large Q^2 ($x_{min} = Q^2/s$) and this $x > 0.2$ cut involves no additional loss of data for $Q^2 > 8000$(GeV/c)^2 for s=40,000 GeV^2.

To estimate the statistical precision of this charge asymmetry measurement, we estimate in rough terms that $\sigma_+ \sim \sigma_-$ and thus $\delta\sigma_+ \sim \delta\sigma_-$ giving

$$A_{ch} \sim \frac{1}{\sqrt{2}} \left(\frac{\delta\sigma}{\sigma}\right)$$

Referring to figure 3, we see that for $Q^2 < 5000$(GeV/c)^2, $A_{ch} \leq 0.4$. Thus to measure the asymmetry to 10% at Q^2 ~5000(GeV/c)^2 requires a 6% measurement of the cross sections σ_+ and σ_-. Hence more than 300 events for each lepton sign are required for $x \geq 0.2$ in that Q^2 bin centered around 5000(GeV/c)^2.

Figure 11 shows the radiative corrected asymmetries for various integrated luminosities. We see that ~10^{39} 1/cm^2 integrated luminosity is needed to determine M_{z^o} to $\pm$20 GeV/c^2. The following table indicates the statistical accuracy of the M_{z^o} determination at M_{z^o}=90 GeV/c^2 for various luminosities. The error on M_{z^o} is at the ± 1 χ^2/df limit.

Table II

Integrated Luminosity for each beam	Mass $\pm$ error (GeV/c^2)
$\int$ Ldt	M_{z^o}
10^{38} cm^{-2}	$90 \pm \begin{matrix}60\\40\end{matrix}$
10^{39} cm^{-2}	$90 \pm \begin{matrix}40\\20\end{matrix}$
10^{40} cm^{-2}	$90 \pm \begin{matrix}10\\5\end{matrix}$

Other ratios can be used to determine M_{z^o}, but they also have a sensitivity to $\sin^2\theta_w$ and are therefore not so straightforward to interpret.

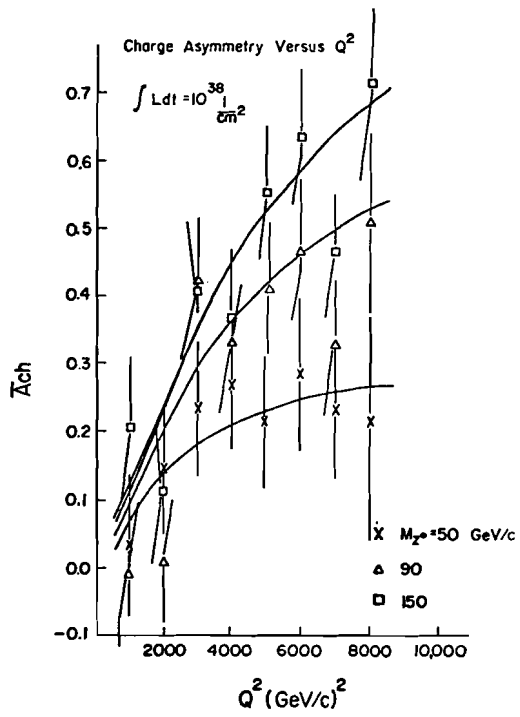

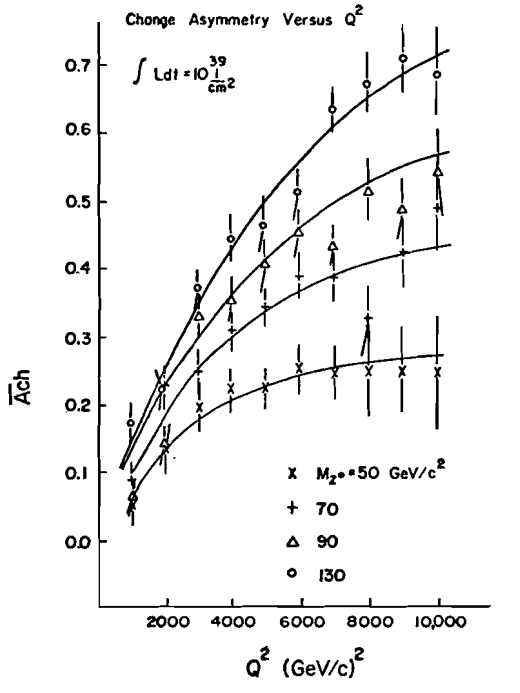

Figure 11: The charge asymmetry versus Q^2 for $S=40000\,(GeV)^2$ for various integrated luminosities per charge of electron beam. The "data" points have been randomly shifted by their respective statistical errors. Radiative corrections have been done.

3) Determination of $\sin^2\theta_w$:

The ratio A_{dLR} given by equation (5) is used to determine $\sin^2\theta_w$. This polarization asymmetry depends on both $\sin^2\theta_w$ and Q^2 and has a very weak x-dependence from the ratio XF_3^{wk}/XF_3^{int} term. No $x \geq 0.2$ cut is required since the Q^2 evolution of XF_3^{int} is expected to be the same as XF_3^{wk}. Hence we may average over X to increase the statistical power of this ratio. In this calculation, the cross sections have been corrected for the approximate radiative correction described above.

The statistical error has been computed by considering both the measured number of "events" and the beam polarization fraction $\rho^{\pm}$. The measured cross section will be the sum of the unpolarized and polarized electron/positron scattering:

$$\sigma_{\mp}^{m} = (1-\rho_{\mp}) \frac{(\sigma_{L\mp} + \sigma_{R\mp})}{2} + \rho_{\mp}\sigma_{\mp}^{pol}$$

for $e^{\mp}$ respectively. Hence the polarized cross sections are determined by:

$$\sigma_{pol\mp} = \frac{1}{\rho_{\mp}}\left[\sigma_{\mp}^{m} - (1-\rho_{\mp}) \frac{(\sigma_{L\mp} + \sigma_{R\mp})}{2}\right]$$

For large $\rho^{\mp} \to 1$, we have the measurement error:

$$\delta\sigma_{pol_{\mp}} \approx \frac{\delta\sigma_{\mp}^{m}}{\rho_{\mp}}$$

The resulting values of A_{dLR} averaged over x as a function of Q^2 with $M_{Z^o}=37.4/\sin\theta_w\cos\theta_w$ required by the standard model is shown in figure 12 for various luminosities. Here we notice that for $\sin^2\theta_w \geq 0.2$, A_{dLR} has very little Q^2 dependence since XF_3^{wk} becomes small for $\sin^2\theta_w$ in that region. We then average over Q^2 to enhance the statistics. This average value of A_{dLR} is shown in figure 13 as a function of $\sin^2\theta_w$ for various luminosities. The average over Q^2 was performed in steps of $\Delta Q^2=1000\ (GeV/c)^2$. Choosing smaller Q^2 steps does not significantly affect the average asymmetry or statistical errors for $\sin^2\theta_w \geq 0.15$. But for $\sin^2\theta_w=0.1$ the average A_{dLR} is smaller for the smaller Q^2 step. Assuming that $\sin^2\theta_w=0.225$, we estimate the following errors:

Table III

$\int Ldt^*$	$(\sin^2\theta_w)$ measured
10^{38} cm^{-2}	0.225 ± 0.022
10^{39} cm^{-2}	0.225 ± 0.007
10^{40} cm^{-2}	0.225 ± 0.002

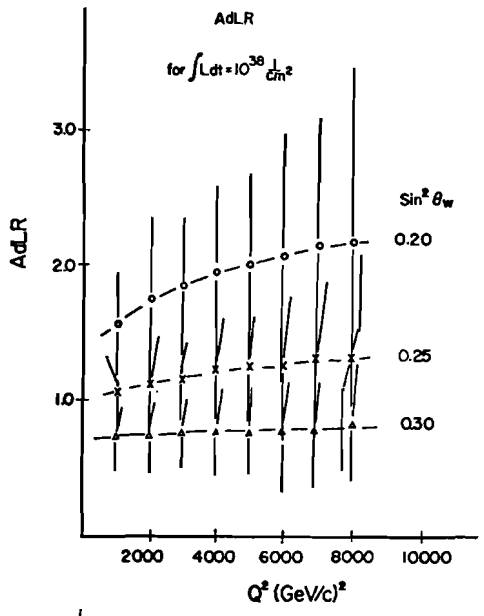

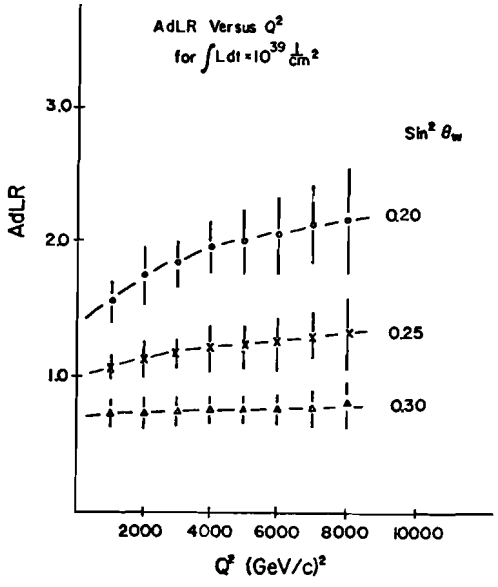

Figure 12: The asymmetry A_{dLR} versus Q^2 for various values of $\sin^2\theta_w$ at several integrated luminosities.

If $\sin^2\theta_w$ happened to depend on Q^2, then A_{dLR} would have an additional Q^2-dependence which could be observed by a deviation from the curves of figure 12. A 10% change in $\sin^2\theta_w$ would be observed for $1000 \leq Q^2 \leq 8000$ $(GeV/c)^2$ for an integrated luminosity of 10^{39} cm^{-2}.

4) Consistency checks of the Standard Model:

The asymmetries $A_{LRe^{\mp}}$ and A_{SLR} given by equation 7 and 9 respectively have a sensitivity to both $\sin^2\theta_w$ and M_{Z^o}, and can therefore be used to check the consistency of the standard model. In this context, $A_{LRe^{\mp}}$ and A_{SLR} are completely determined by the measurement of $\sin^2\theta_w$, (and M_{Z^o} - if we choose M_{Z^o} as an independent parameter).

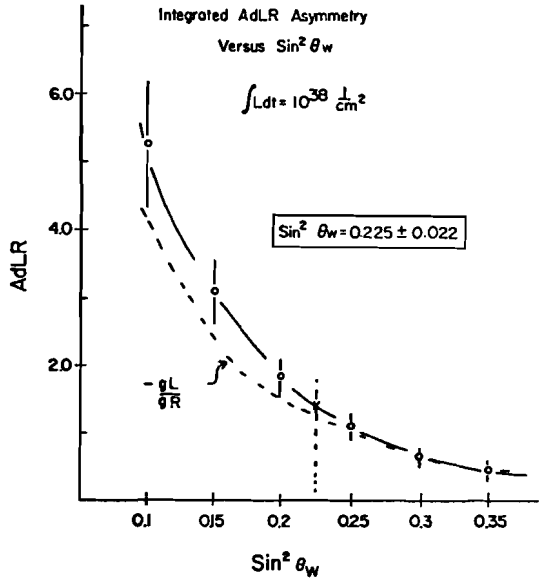

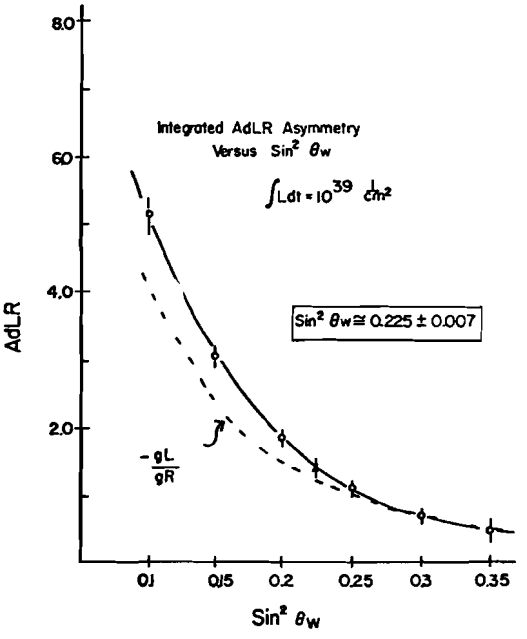

Figure 13: The A_{dLR} asymmetry integrated over X and Q^2 in steps of ΔQ^2=1000 $(GeV/c)^2$ versus $\sin^2\theta_w$ for various integrated luminosities. The value at $\sin^2\theta_w \approx 0.1$ is somewhat dependent on the Q^2 step size since at this value of $\sin^2\theta_w$, the asymmetry A_{dLR} has a Q^2-dependence. The Q^2=0 value of this ratio is shown as the dotted line. The error bars are for the polarization=80%.

In figure 14 we plot A_{LRe^-} versus Q^2 for various values of the integrated luminosity. The corresponding plot for A_{LRe^+} is shown in figure 15. These plots have the approximate radiative corrections and errors computed as above. We see that for $\int Ldt \approx 10^{39}/cm^2$, the A_{LRe^-} ratio can be used to measure $\sin^2\theta_w$ to $\sim \pm 0.03$. The A_{LRe^+} ratio has less sensitivity.

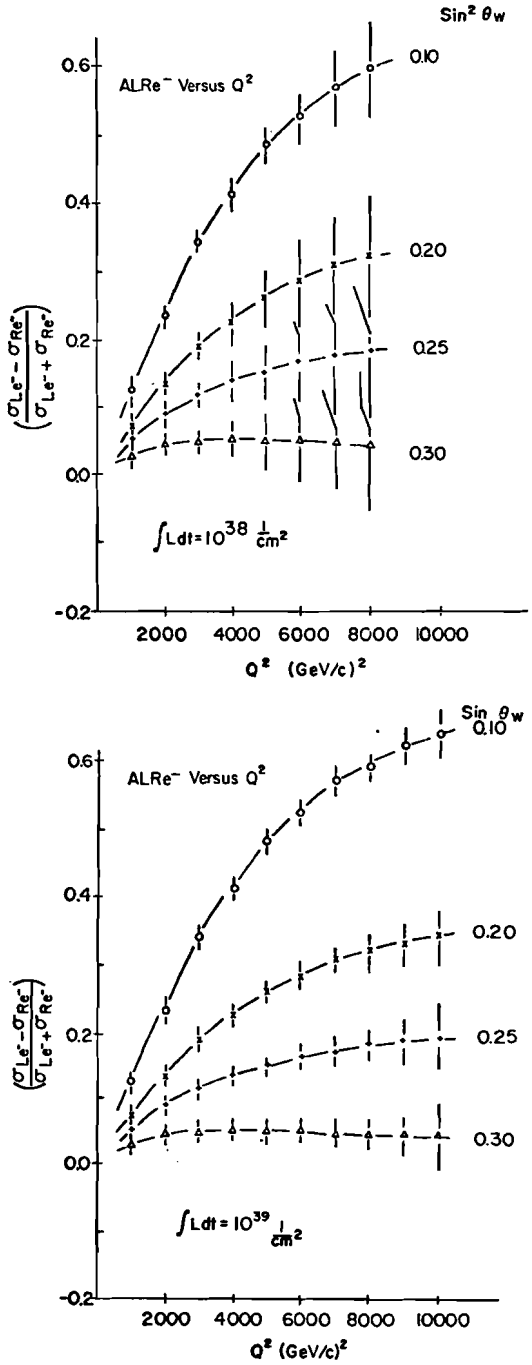

Figure 14: The asymmetry A_{LRe^-} versus Q^2 for various values of $\sin^2\theta_w$ for several values of integrated luminosities. The z^o mass is assumed to depend on $\sin^2\theta_w$ according to the standard model.

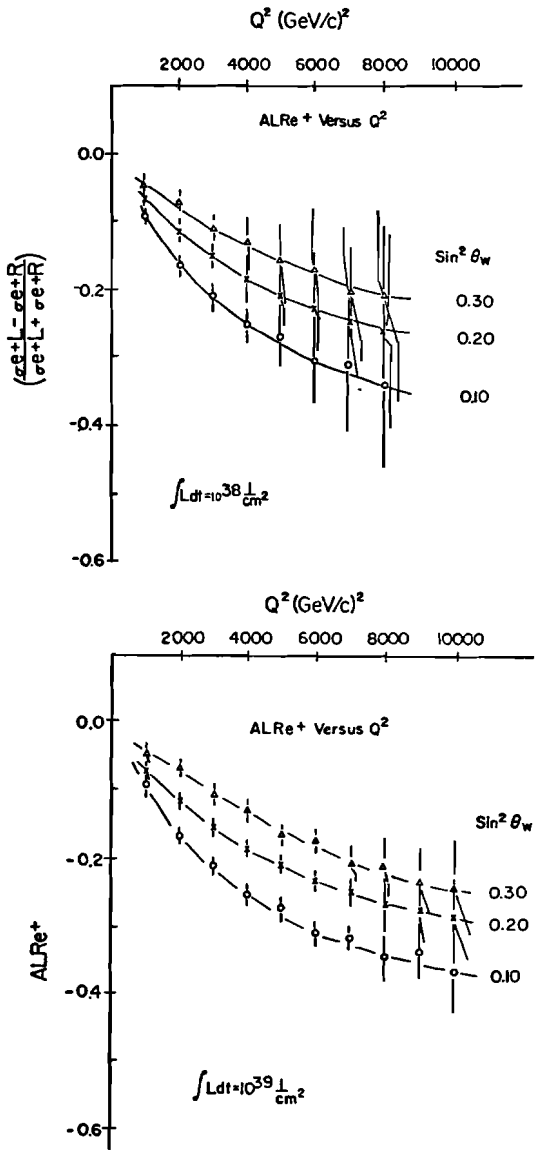

Figure 15: The asymmetry A_{LRe^+} versus Q^2 for various values of $\sin^2\theta_w$ and integrated luminosities.

The sum asymmetry A_{SLR} is plotted in figure 16 for various integrated luminosities. For $\int Ldt \sim 10^{39}/cm^2$, we can measure $\sin^2\theta_w$ to ± 0.03. Since this ratio has no radiative corrections, it offers an important test of all of the other asymmetries discussed above.

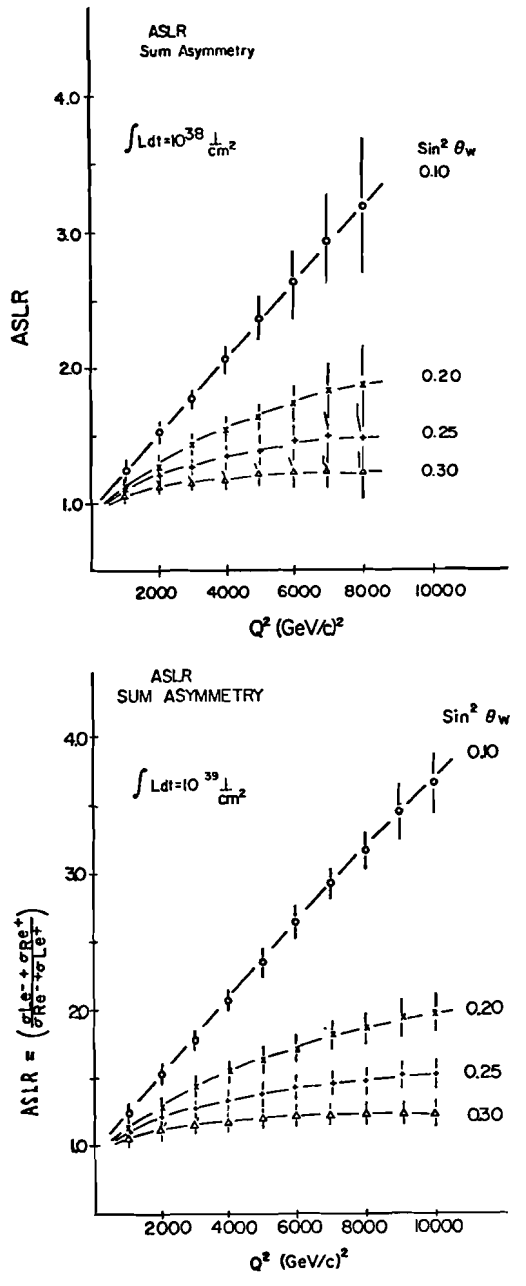

Figure 16: The sum asymmetry A_{SLR} versus Q^2 for various values of $\sin^2\theta_w$ for various integrated luminosities. Note that this ratio is independent of the radiative 1γ-2γ interference effect.

(VI) Conclusions:

An ep collider can offer stringent tests of the standard SU(2)xU(1) model electro weak interactions. The primary advantage of this experiment is that these tests can be performed at high Q^2 where possible deviations might be observed through a Q^2-dependence of $\sin^2\theta_w$. Several points are worth noting:

1. The 2γ-1γ radiative effect is large compared to the expected asymmetry from weak interaction effects. Thus a measurement of the radiative effect is essential. This requires a measurement of $e^{\pm}$-p scattering at low $Q^2 (40 \leq Q^2 \leq 400\,(GeV/c)^2)$ and the detector should be able to accommodate this requirement.

2. It is necessary to impose an $x > 0.2$ cut in using the charge asymmetry to determine the Z^o mass by the propagator effect. This limits the statistics of this measurement somewhat and requires that $\int Ldt \geq 10^{39}/cm^2$ for a useful measurement of M_{Z^o} to be made.

3. The parameter $\sin^2\theta_w$ can be determined by the asymmetry A_{dLR}. Since this ratio involves $e^- - e^+$ cross section differences, it is severly distorted by the radiative effect described above. With this effect corrected, a measurement of $\sin^2\theta_w$ to $< 10\%$ is possible.

4. Important consistency checks of the standard model can be made with asymmetries which depend on both $\sin^2\theta_w$ and M_{Z^o}.

5. The quality of these measurements are far more dependent on the degree of beam polorization and the integrated luminosity than on S. It is important to have enough luminosity to make precise measurements in the $Q^2 > 6000\,(GeV/c)^2$ range. Roughly $> 10^{39}/cm^2$ is required for this.

Acknowledgement

Conversations with J. Morphin, M. Shaevitz, J. Friedman, D.H. White, C. Albright, G. Tenachas are gratefully acknowledged.

References:

1. C.Y. Prescott, et al.; P.L. 77B , 524, (1978) and C.Y. Prescott, et al.; P.L. 84B , 524, (1979).
2. M. Klein and T. Riemann; P.L. 76B , 70 (1978 and M. Klein, T. Riemann, I.A. Savin; P.L. 85B , 385 (1979).
3. J. D. Bjorken, SLAC-PUB-2062 (1977) ;Phys. Rev. 19D, 335, (1979)
4. P.Q. Hung and J.J. Sakurai, N.P. B143 , 81 (1978).
5. N. Dombey, Neutrino-79, Bergen, Norway p.645 (1979).
6. CHEEP proposal - CERN 78-02; P-659 (W. Lee and R.R. Wilson - Cospokesmen).

7. A.J. Buras and K.J.F. Gaemers; N.P. B132 , 249 (1978).

8. V.G. Gorshkov, et al., Yad. Phys. (USSR) 6, 129 (1967).

9. J. Bartels; N.P. B82 , 172, (1974).

10. P.M. Fishbane and R.L. Kingsley; Phys. Rev. 8D , 3074 (1973).